PACKAGING STUDY FOR A 512-CHANNEL INTRAOCULAR EPIRETINAL IMPLANT

Jay Han-Chieh Chang[1], *Yang Liu*[1], *Dongyang Kang*[1], *Manuel Monge*[1], *Yu Zhao*[1], *Chia-Chen Yu*[1], *Azita Emami-Neyestanak*[1], *James Weiland*[2], *Mark Humayun*[2], *and Yu-Chong Tai*[1]
[1]California Institute of Technology, CA, USA
[2]Doheny Retina Institute at the Doheny Eye Institute, University of Southern California, CA, USA

ABSTRACT

Much effort has been put into developing multi-channel retinal prosthetic devices. Currently, even the most advanced prostheses do not have enough channels to provide vision to a desirable level. In this paper, we present a system design and a packaging scheme for a 512-channel intraocular epiretinal implant. Both a wireless power coil (with high transfer efficiency) and a data coil are included for this intraocular system. Simulation of the interference between coils is investigated and the results show that the two coils can be put in a co-planar fashion using two notch filters to minimize interference. The complete package is demonstrated with a mechanical model with a parylene-C flexible circuit board, i.e., parylene flex, to show the placement of the IC chips, discrete components, and coils. It also shows the final folded device after surgical insertion into an eye to save space. The feasibility of the proposed structure has been successfully tested *in vivo*. Experimentally, the maximum allowable pulling force is measured by a dynamic mechanical analysis (DMA) machine to be 8N, which provides a large safety margin for surgery.

INTRODUCTION

Two of the most common retinal degenerative diseases worldwide are the age-related macular degeneration (AMD) and retinitis pigmentosa (RP). Several millions of people are estimated to be affected by these two diseases in the next ten years [1-2]. Blurry central vision and tunnel vision are the typical symptoms of the two diseases respectively, as shown in Figure 1. Even though gene therapies, drug and nutritional therapies [3-4] have been and are being developed to decrease the rate of such occurrence, the two diseases still cause the loss of rod and cone receptors in the eye in the long run and blindness becomes inevitable. Visual prosthesis, a technology aiming to solve these problems and to regain eyesight for AMD and RP patients, then becomes a feasible current choice for research and development around the world. Many groups have effort to develop multi-electrode arrays for retinal prosthetic applications [5-6]. However, even the most advanced prostheses do not have enough stimulating channels to restore vision to the desirable functional capability, like facial recognition or large-sized letter reading. Currently, the most advanced retinal implant approved by Food and Drug Administration (FDA) is the Second Sight's 60-channel Argus II implant [7]. However, this technology has not yet reached the minimally desirable number of channels around 1,000.

In this paper, a system design and its packaging for a 512-channel epiretinal implant is presented using a parylene flex technology. A special 3-coil (i.e., two extraocular and one intraocular coils) wireless power transfer system with high efficiency up to 36.5% and a separate intraocular data coil are employed for this system. The two intraocular power and data coils are arranged in a co-planar fashion to save space due to surgical consideration. An implant mechanical model, i.e., a real device but without real IC chips, connected with dummy chips, discrete components (i.e., capacitors, inductors, and resistors) and two intraocular coils is optimized for component placement and surgical insertion into an eye. The maximum surgically allowable pulling force of the proposed epiretinal implant is measured using creep test by a DMA machine to be 8N, which provides a large safety margin for surgery. Note that the following work is ongoing for a real implant with working IC chips. The IC chips are independently developed by Manuel Monge et al. from the Mixed-mode Integrated Circuits and Systems group at Caltech. Details of the chip will be published in ISSCC 2013 [8].

Figure 1. (a) Normal vision; (b) Blurry central vision for AMD patients; (c) Tunnel vision for RP patients.

FABRICATION AND INTERGRATON

A. PARYLENE FLEX

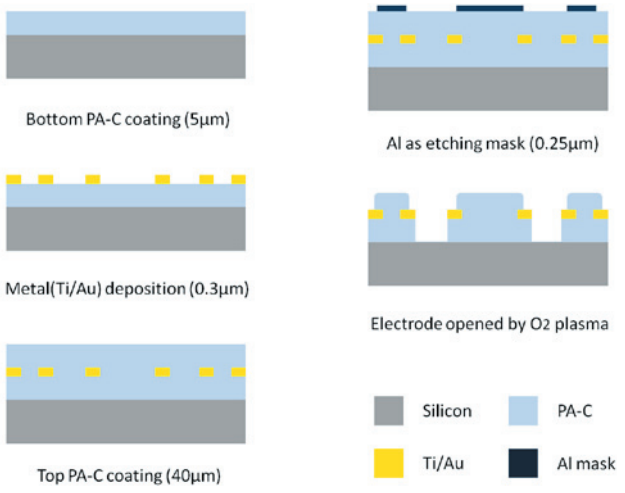

Figure 2. Fabrication process of the parylene-C flexible circuit board.

The fabrication process of the parylene-C flexible circuit board, i.e., parylene flex, started with a 5μm parylene-C deposition on HMDS treated silicon wafers, which will help the parylene flex to be released from DI water in the last step, as shown in Figure 2. The parylene deposition was followed by a Ti/Au (~0.3μm) metal lift-off process to provide electrical connection. A second and the top thick parylene-C (~40μm) was then deposited to complete the parylene-metal–parylene sandwich skin structure. Aluminum (0.25μm) was deposited as the parylene-C etching mask to etch through thick parylene-C interfaces. Finally, electrode sites and the device contour were then defined by a two-step O2 plasma etching.

B. HIGH-DENSITY MULTI-CHANNEL CHIP INTEGRATION

A previously developed high yield and high-density multi-channel chip connection technique [9, 10] was used to make connection of this work. The parylene flex was first aligned with IC chips under microscope. An alignment accuracy of around 10 μm was achieved. A conductive epoxy squeegee technique, as shown in Figure 3, was then applied to make electrical and mechanical connections for the epiretinal prosthesis integration. A commercially available conductive epoxy (MG Chemicals) was first mixed and applied on the surface of the edge of the parylene flex. The parylene flex has holes and wells that were etched during the fabrication process which acted as the screen for this squeegee process. A rubber squeegee was then used to push the epoxy across surface so the epoxy filled the wells in the parylene flex, and electrically connected the electrical traces that were embedded inside the parylene flex and the bonding pads on the chips together.

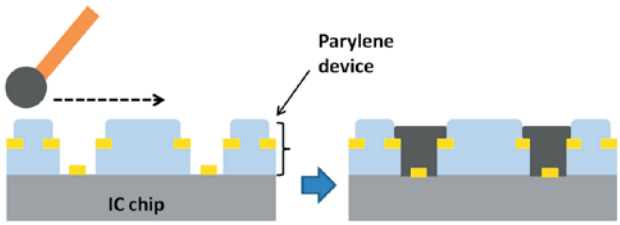

Figure 3. Demonstration of the process flow of conductive epoxy squeegee technique to make electrical and mechanical connections between parylene flex and chips.

3-COIL WIRELESS POWER TRANSFER AND DATA COIL INTERFERENCE

A. 3-COIL WIRELESS POWER TRANSFER

To wirelessly power the whole epiretinal system, a 3-coil wireless power transfer system is used as shown in Figure 4. The flexible and foldable MEMS intraocular foil receiver coil, L3 in Figure 4, features a Q factor of 24 (at the operating frequency of 10MHz), a diameter of 10mm and a weight of 10mg in saline [11]. This coil is placed inside the lens capsule. The intermediate coil, L2, is a hand-wounded Litz buffer coil to enhance coupling coefficients κ12 and κ23 due to its high Q factor and close proximity to receiver coil. Because of the additional intermediate coil, the overall power transfer efficiency of the design was measured to be as high as 36.5% with one inch separation between the primary transmitter coil, L1, and the intraocular receiver coil, L3.

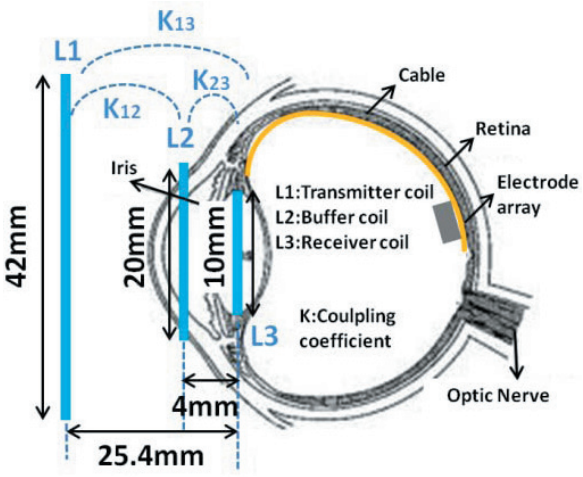

Figure 4. The 3-coil scheme for inductive power transfer.

B. SIMULATION OF INTERFERENCE BETWEEN COILS

For surgical and placement consideration, it is the best to have the power and data coils in a co-planar fashion. However, the co-planar placement has the largest interference issue between the power and data coils. To analyze the interference between power and data coils, a model of the coil system was built using high frequency structural simulator (HFSS), as shown in Figure 5. Coil 1 is defined as the receiver coil of the data coil, with 3mm, 5mm, and 7mm inner diameter; coil 2 is defined as the receiver coil of the intraocular power coil, with 10mm inner diameter; coil 3 is defined as the transmitting data coil, with 20mm in diameter; coil 4 is defined as the transmitting power coil, with 42mm in diameter. The thickness of the coils is 2mm and the separation between the receiving and transmitting coils is set to be one inch.

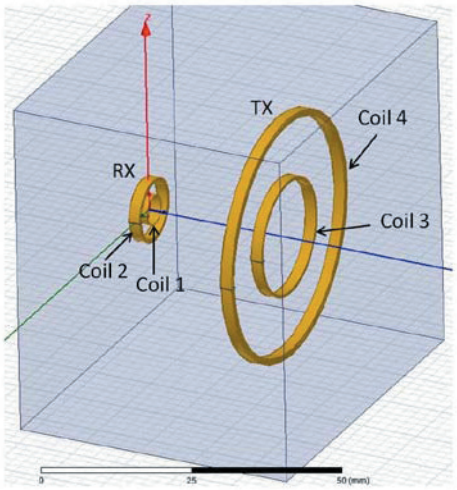

Figure 5. A model of the coil system is built using HFSS for the coil interference analysis.

Figure 6 shows the simulation result. Scattering parameters (S-parameters), describing the electrical behavior of linear electrical networks, from coil 4 to coil 1 and from coil 3 to coil 1 were simulated for us to estimate the interference between power and data coils. The resonating capacitors are 30pF for coil 1, 700pF for coil 2 and coil 3, and 600pF for coil 4. At the frequency of 160MHz where the data coil operates, an interference signal at 10MHz coming from the power coil will cause a 20dB higher coupling compared to the data coil.

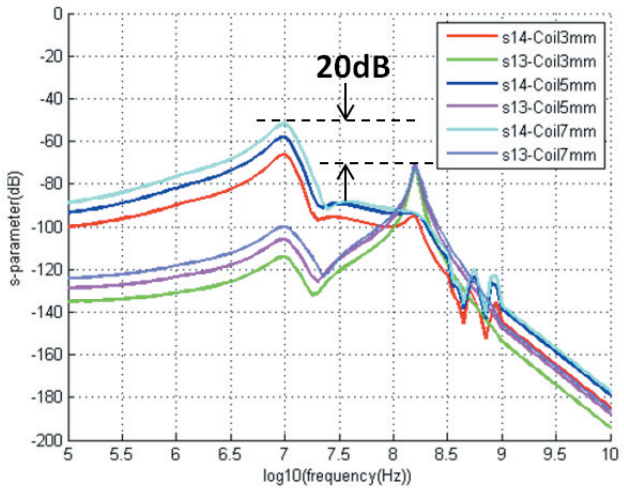

Figure 6. S-parameters from coil 4 to coil 1 and from coil 3 to coil 1 with different inner diameters of coil 1.

In order to reduce interference from the power coil to the data coil, two notch filters, as shown in Figure 7, were added to the circuit. The notch filters, built by RLC circuits, can decrease the coupling in the data path. They reduce the coupling at 10MHz (i.e., the power transfer frequency), making possible to demodulate data at 160MHz. It is also possible to tune the resonant frequency to increase the gain at 160MHz which will be better for data transfer. The only drawback is that 6 more extra discrete components will be added to the whole system. However, our surgical design can tolerate this issue so that not too much volume will be added to the device.

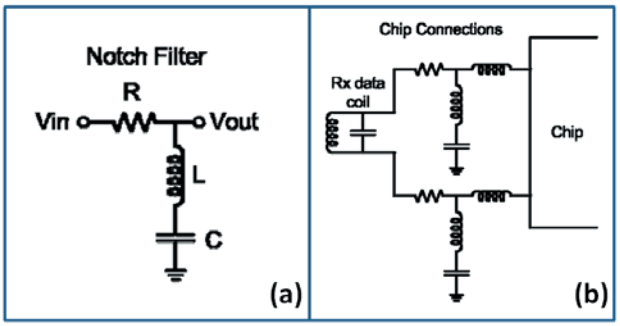

Figure 7. (a) a Notch filter. (b) Two Notch filters are connected to the system.

THE FLEXIBLE MECHANICAL MODEL

The surgical procedure for the insertion and fixation of the implant is very important. To this end, a parylene flex mechanical model was designed and fabricated, as shown in Figure 8, to be packaged with silicon chips, discrete components (including capacitors, inductors, and resistors), and coils. A mold was designed to house the silicon chips for one-time conductive epoxy squeegee connection process to increase the connection yield. All the discrete components were placed on a parylene flex tail. A single retinal tack hole (100µm in diameter) and two suture holes (2mm in diameter) were also designed for the implant to be fixed on designated tissues inside eyeball. Biocompatible silicone was used for further protection after all the process [12]. Based on the high flexibility of the parylene flex implant and low interference between power and data coils with notch filters, the parylene tail can be wrapped around the chips and the coils can be put together in a co-planar fashion, which will be beneficial for surgical insertion and placement. The packaging shown here is based on a two-chip master/slave architecture with two notch filters (built by 6 discrete components), and 17 discrete components. However, the final goal of on-going chip development is to have only one single IC chip and fewer discrete components.

The current mechanical model, as shown in Figure 9, has been tested for *in vivo* implantation at the Keck School of Medicine of the University of Southern California. The size of the model can fit the pig's eyeball well without damaging the tissues, and the part of the stimulating electrode can reach the retina.

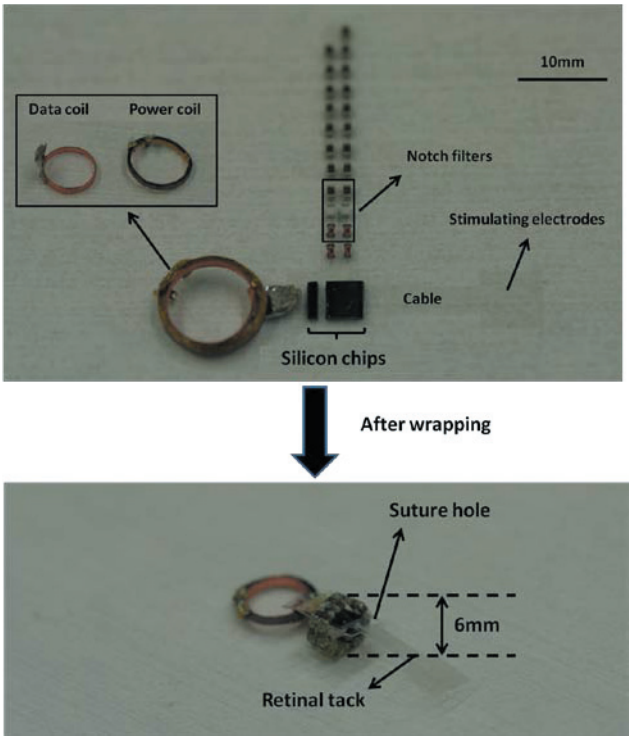

Figure 8. Demonstration of a parylene flex mechanical model before and after wrapping with silicon chips, discrete components, and coils.

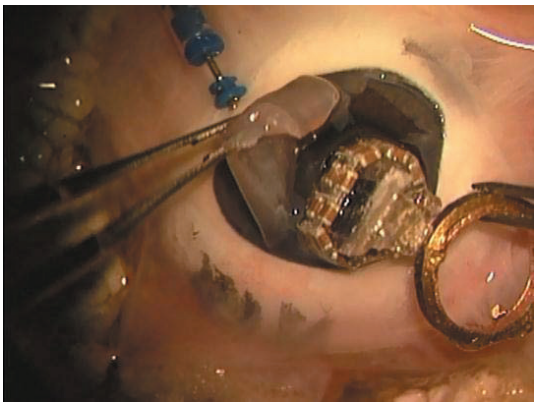

Figure 9. Successful in vivo implantation process in a pig's eye.

MAXIMUM PULLING FORCE

In order to ensure that the parylene flex survives possible large surgical forces, maximum pulling forces on our parylene flex substrates were tested, as shown in Figure 10, using a dynamic mechanical analysis (DMA) machine Q800 from TA instruments [13-14]. The size of the samples was designed to be 5mm by 10mm to fit the geometry factor of the machine. Creep test with a constant loading stress at body temperature of 37ºC was performed on the samples. Before the creep test started, we waited for 30 minutes of sample soaking in saline to ensure that the thermal equilibrium with the targeted temperature. Then, a constant stress was applied onto the samples for 10 minutes to measure the changes of the strain. The stress was then removed for 10 minutes to observe the recovery behavior. The maximum strain of the samples is measured to be 2.7% at an applied stress of 33.2MPa. In brief, the samples can burden an applied force as high as 8N during surgery, which is confirmed by our collaborating surgeons to be a very large safety margin for surgical handling. The additional parylene and silicone protection coating is believed to further increase the maximum allowable force.

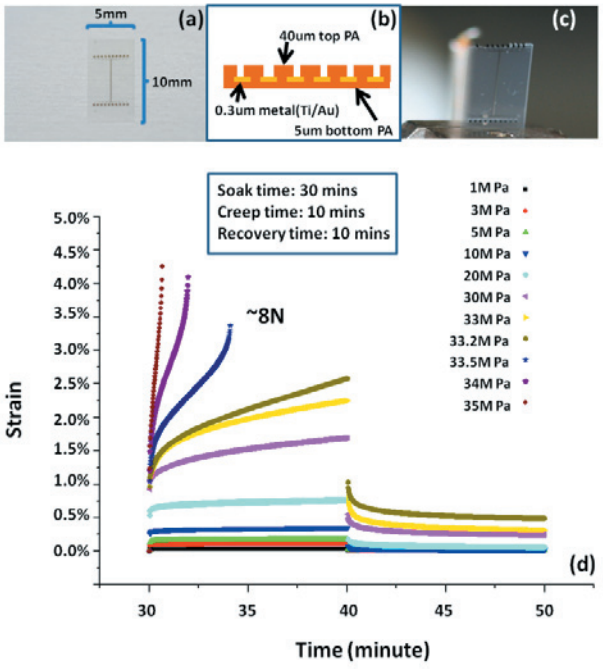

Figure 10. (a) Parylene flex test sample. (b) Cross-section of the tested sample. (c) Broken sample caused by over-stress. (d) Creep test at body temperature of 37°C.

CONCLUSION

A proposed packaging for a 512-channel epiretinal implant was presented here. The 3-coil wireless power transfer system with high transfer efficiency and data coils were included in this system. Simulation of the coil interference by Cadence was investigated and analyzed to show that adding two notch filters could solve the interference issues.

Accordingly, a parylene flex implant model was designed and fabricated to include the chips, discrete components, and coils. In the model, the power and data coils were put in a coplanar fashion. Also, there was a parylene flex tail with all discrete components and later the tail was wrapped around the chips. The maximum allowable pulling force of the parylene flex was also measured by a DMA machine to be 8N, which provides a large safety margin for surgery.

ACKNOWLEDGEMENTS

This work is supported by Biomimetic MicroElectronic Systems (BMES). The authors would also like to thank Mr. Trevor Roper and other lab members of the Caltech Micromachining Laboratory for assistance with fabrication and fruitful discussion.

REFERENCES

[1] Bo Lu et al., *Biomedical Microdevices*, vol. 14, pp. 659-667, 2012
[2] Bo Lu et al., *Proc. TRANSDUCER 2011,* pp. 950-953.
[3] E. W. D. Norton et al., *Arch Ophthalmol*, vol. 11, pp. 1460-1463, 1993
[4] J. Bennett et al., *Nature Medicine*, vol. 2, pp. 649-654, 1996
[5] T. Stieglitz, *Journal of Neural Engineering*, vol. 6, 065005
[6] L. Theogarajan et al., *Proc. VLSI-DAT 2009,* pp. 126-129.
[7] Second Sight (www.2-sight.com)
[8] M. Monge et al., to appear in the Digest of tech. papers, ISSCC 2013
[9] Jay H.C. Chang et al., *Proc. MEMS 2012,* pp. 353-356.
[10] Jay H.C. Chang et al., *Proc. TRANSDUCER 2011,* pp. 390-393.
[11] Yu Zhao et al., *Proc. TRANSDUCER 2011,* pp. 2172-2175.
[12] Wendian Shi et al., *Proc. TRANSDUCER 2009,* pp. 616-619.
[13] J. C. Lin et al., *Proc. TRANSDUCER 2011,* pp. 2698-2701.
[14] Wendian Shi et al., *Sensors & Actuators A: Physical*, vol. 130-131, pp. 352-357, 2006.

CONTACT

*Jay Han-Chieh Chang, tel: +1-626-379-3313; jaychang@caltech.edu